MID-OCEAN RIDGES: MANTLE CONVECTION AND FORMATION OF THE LITHOSPHERE

G. Ito and R. A. Dunn, University of Hawai'i at Manoa, Honolulu, HI, USA

Introduction

Plate tectonics describes the motion of the outer lithospheric shell of the Earth. It is the surface expression of mantle convection, which is fueled by Earth's radiogenic and primordial heat. Mid-ocean ridges mark the boundaries where oceanic plates separate from one another and thus lie above the upwelling limbs of mantle circulation (Figure 1). The upwelling mantle undergoes pressure-release partial melting because the temperature of the mantle solidus decreases with decreasing pressure. Newly formed melt, being less viscous and less dense than the surrounding solid, segregates from the residual mantle matrix and buoyantly rises toward the surface, where it forms new, basaltic, oceanic crust. The crust and mantle cool at the surface by thermal conduction and hydrothermal circulation. This cooling generates a thermal boundary layer, which is rigid to convection and is the newly created edge of the tectonic plate. As the lithosphere moves away from the ridge, it thickens via additional cooling, becomes denser, and sinks deeper into the underlying ductile asthenosphere. This aging process of the plates causes the oceans to double in depth toward continental margins and subduction zones (Figure 2), where the oldest parts of plates are eventually thrust downward and returned to the hot underlying mantle from which they came.

Mid-ocean ridges represent one of the most important geological processes shaping the Earth; they produce over two-thirds of the global crust, they are the primary means of geochemical differentiation in the Earth, and they feed vast hydrothermal systems

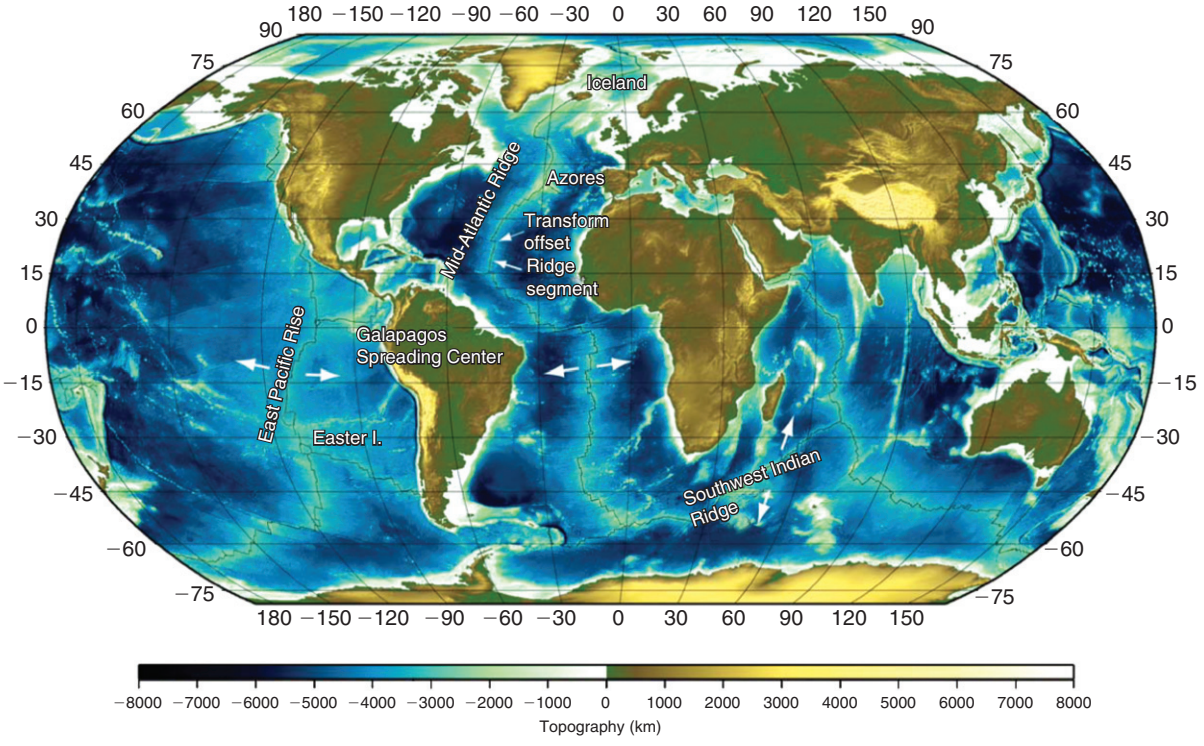

Figure 1 Map of seafloor and continental topography. Black lines mark the mid-ocean ridge systems, which are broken into individual spreading segments separated by large-offset transform faults and smaller nontransform offsets. Mid-ocean ridges encircle the planet with a total length exceeding 50 000 km. Large arrows schematically show the direction of spreading of three ridges discussed in the text.

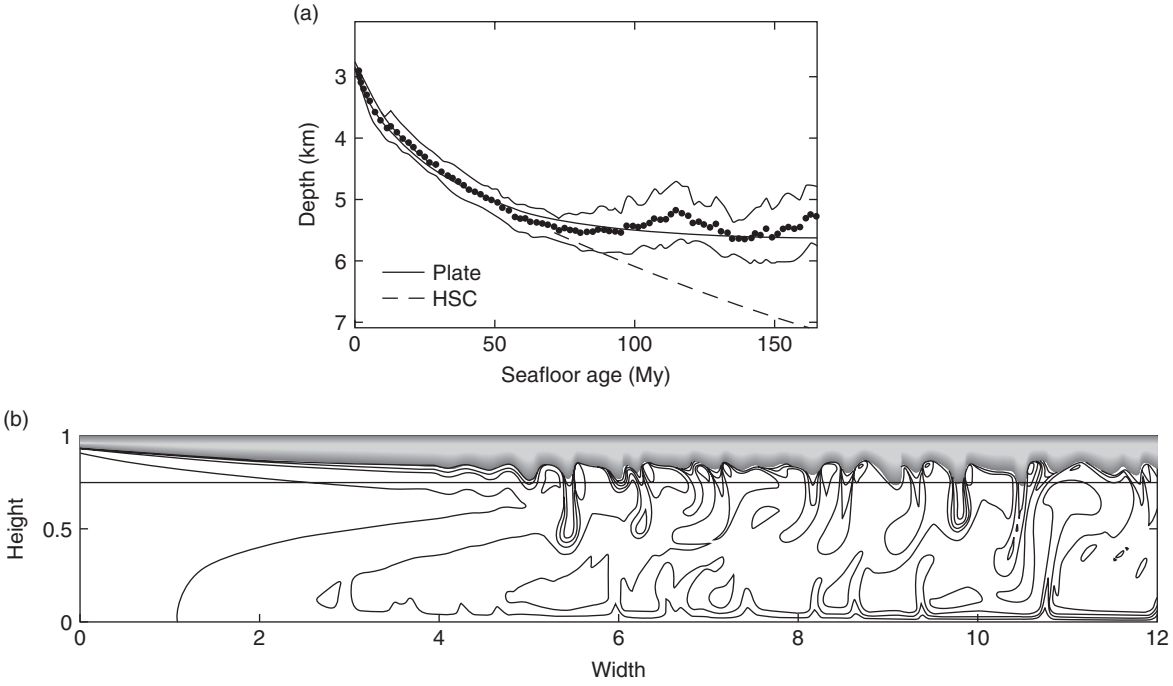

Figure 2 (a) Global average (dots) seafloor depth (after correcting for sedimentation) and standard deviations (light curve) increase with seafloor age. Dashed curve is predicted by assuming that the lithosphere cools and thickens indefinitely, as if it overlies an infinite half space. Solid curve assumes that the lithosphere can cool only to a maximum amount, at which point the lithosphere temperature and thickness remain constant. (b) Temperature contours in a cross section through a 2-D model of mantle convection showing the predicted thickening of the cold thermal boundary layer (i.e., lithosphere, which beneath the oceans reaches a maximum thickness of ~100 km) with distance from a mid-ocean ridge (left side). Midway across the model, small-scale convection occurs which limits the thickening of the plate, a possible cause for the steady depth of the seafloor beyond ~80 Ma. (a) Modified from Stein CA and Stein S (1992) A model for the global variation in oceanic depth and heat flow with lithospheric age. *Nature* 359: 123–129, with permission from Nature Publishing Group. (b) Adapted from Huang J, Zhong S, and van Hunen J (2003) Controls on sublithospheric small-scale convection. *Journal of Geophysical Research* 108 (doi:10.1029/2003JB002456) with permission from American Geophysical Union.

that influence ocean water chemistry and support enormous ecosystems. Around the global ridge system, new lithosphere is formed at rates that differ by more than a factor of 10. Such variability causes large differences in the nature of magmatic, tectonic, and hydrothermal processes. For example, slowly spreading ridges, such as the Mid-Atlantic Ridge (MAR) and Southwest Indian Ridge (SWIR), exhibit heavily faulted axial valleys and large variations in volcanic output with time and space, whereas faster-spreading ridges, such as the East Pacific Rise (EPR), exhibit smooth topographic rises with more uniform magmatism. Such observations and many others can be largely understood in context of two basic processes: asthenospheric dynamics, which modulates deep temperatures and melt production rates; and the balance between heat delivered to the lithosphere, largely by magma migration, versus that lost to the surface by conduction and hydrothermal circulation. Unraveling the nature of these interrelated processes requires the integrated use of geologic mapping, geochemical and petrologic analyses, geophysical sensing, and geodynamic modeling.

Mantle Flow beneath Mid-ocean Ridges

While the mantle beneath mid-ocean ridges is mostly solid rock, it does deform in a ductile sense, very slowly on human timescales but rapidly over geologic time. 'Flow' of the solid mantle is therefore often described using fluid mechanics. The equation of motion for mantle convection comes from momentum equilibrium of a fluid with shear viscosity η and zero Reynolds number (i.e., zero acceleration):

$$\nabla \bullet \left[\eta\left(\nabla \mathbf{V} + \nabla \mathbf{V}^T\right)\right] - \nabla P + \nabla[(\zeta - 2/3\eta)\nabla \bullet \mathbf{V}] + (1-\phi)\Delta\rho\mathbf{g} = 0 \quad [1]$$

The first term describes the net forces associated with matrix shear, where $\mathbf{V}$ is the velocity vector, $\nabla\mathbf{V}$ is the velocity gradient tensor, and $\nabla\mathbf{V}^T$ is its transpose; the second term ∇P is the non-hydrostatic pressure gradient; the third term describes matrix divergence $\nabla \bullet \mathbf{V}$ (with effective bulk viscosity ζ) associated with melt transport; and the last term is the body force, with ϕ being the volume fraction occupied by melt

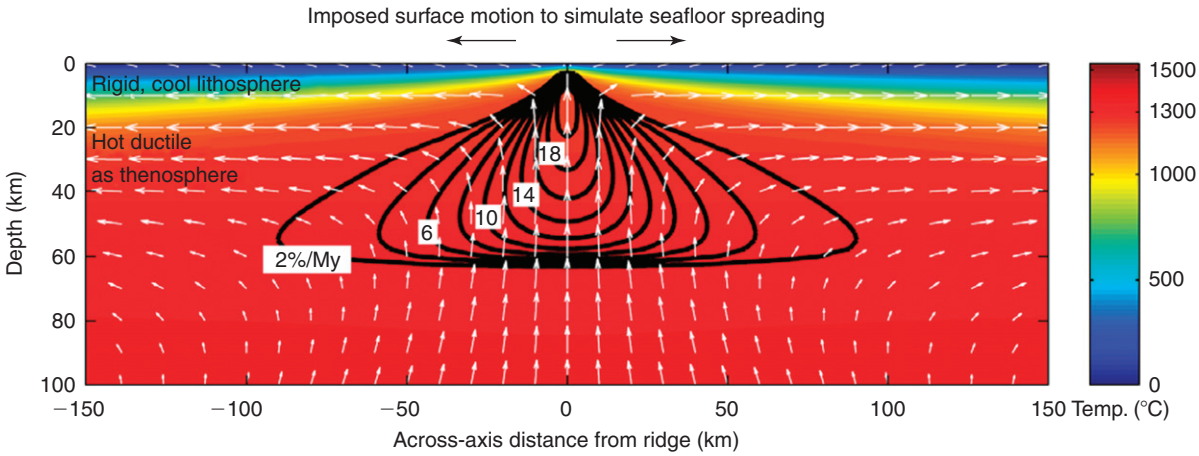

Figure 3 Cross section of a 2-D numerical model that predicts mantle flow (shown by arrows whose lengths are proportional to flow rate), temperatures (shading), and melt production rate beneath a mid-ocean ridge (contoured at intervals of 2 mass %/My). In this particular calculation, asthenospheric flow is driven kinematically by the spreading plates and is not influenced by density variations (i.e., mantle buoyancy is unimportant). Model spreading rate is 6 mm yr^{-1}.

and $\nabla\rho$ being the density contrast between the solid and melt. To first order, the divergence term is negligible, in which case eqn [1] describes a balance between viscous shear stresses, pressure gradients, and buoyancy. Locally beneath mid-ocean ridges, the spreading lithospheric plates act as a kinematic boundary condition to eqn [1] such that seafloor spreading itself drives 'passive' mantle upwelling, which causes decompression melting and ultimately the formation of crust (Figure 3). Independent of plate motion, lateral density variations can drive 'active' or 'buoyant' mantle upwelling and further contribute to decompression melting, as we discuss below.

Several lines of evidence indicate that the upwelling is restricted to the upper mantle. The pressures at which key mineralogical transitions occur in the deep upper mantle (i.e., at depths 410 and 660 km) are sensitive to mantle temperature, but global and detailed local seismic studies do not reveal consistent variations in the associated seismic structure in the vicinity of mid-ocean ridges. This finding indicates that any thermal anomaly and buoyant flow beneath the ridge is confined to the upper mantle above the discontinuity at the depth of 410 km. Regional body wave and surface wave studies indicate that it could even be restricted to the upper ~200 km of the mantle. Although some global tomographic images, based on body wave travel times, sometimes show structure beneath mid-ocean ridges extending down to depths of 300–400 km, these studies tend to artificially smear the effects of shallow anomalies below their actual depth extent. Further evidence comes from the directional dependence of seismic wave propagation speeds. This seismic anisotropy is thought to be caused by lattice-preferred orientation of olivine crystals due to mantle flow. Global studies show that at depths of 200–300 km beneath mid-ocean ridges, surface waves involving only horizontal motion (Love waves) tend to propagate slower than surface waves involving vertical motion (Rayleigh waves). This suggests a preferred orientation of olivine consistent with vertical mantle flow at these depths but not much deeper.

Mantle Melting beneath Mid-ocean Ridges

Within the upwelling zone beneath a ridge, the mantle cools adiabatically due to the release of pressure. However, since the temperature at which the mantle begins to melt drops faster with decreasing pressure than the actual temperature, the mantle undergoes pressure-release partial melting (Figure 3). In a dry (no dissolved H_2O) mantle, melting is expected to begin at approximately 60-km depth. On the other hand, a small amount of water in the mantle ($\sim 10^2$ ppm) will strongly reduce the mantle solidus such that melting can occur at depths >100 km. Detailed seismic studies observe low-velocity zones extending to depth of 100–200 km, which is consistent with the wet melting scenario.

The thickness of oceanic crust times the rate of seafloor spreading is a good measure of the volume flux (per unit length of ridge axis) of melt delivered from the mantle. Marine seismic studies of the Mohorovičić seismic boundary (or Moho), which is often equated with the transition between the

gabbroic lower oceanic crust and the peridotitic upper mantle, find that the depth of the Moho is more or less uniform beneath seafloor formed at spreading rates of $\sim 20\,\mathrm{mm\,yr^{-1}}$ and faster (Figure 4). This observation indicates that the flux of melt generated in the mantle is, on average, proportional to spreading rate. What then causes such a behavior? Melt flux is proportional to the height of the melting zone as well as the average rate of upwelling within the melting zone. If the upwelling and melt production rate are proportional to spreading rate, then, all else being equal, this situation explains the invariance of crustal thickness with spreading rate. On the other hand, all else is not likely to be equal: slower spreading tends to lead to a thicker lithospheric boundary layer, a smaller melting zone, and a further reduction in melt production. The cause for the lack of decrease in

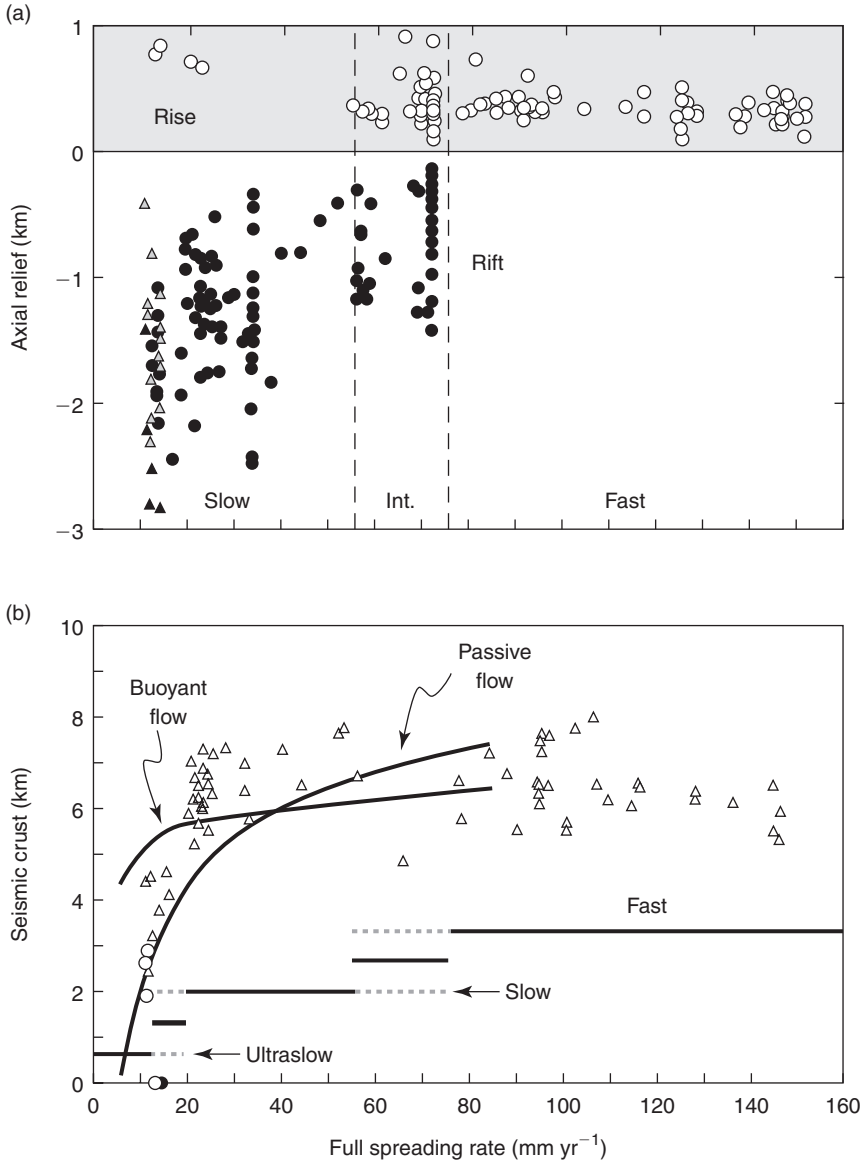

Figure 4 (a) Axial morphology of ridges is predominantly rifted valleys (negative relief) along slow-spreading ridges and axial topographic highs (positive relief) along fast-spreading rates. The ultraslow spreading ridges (triangles) include the Gakkel Ridge in the Arctic and South West Indian Ridge, southeast of Africa. Dashed lines show conventional divisions between slow-, intermediate-, (labeled 'Int.'), and fast-spreading ridges. (b) Seismically determined crustal thicknesses (symbols) are compared to theoretical predictions produced by two types of mantle flow and melting models: the passive flow curve is for a mantle flow model driven kinematically by plate spreading, the buoyant flow curve includes effects of melt buoyancy, which enhances upwelling and melting, particularly beneath slow-spreading ridges. Horizontal bars show a revised classification scheme for spreading rate characteristics. Reprinted by permission from Macmillan Publishers Ltd: *Nature* (Dick HJB, Lin J, and Schouten H (2003) An ultraslow-spreading class of ocean ridge. *Nature* 426: 405–412), copyright (2003).

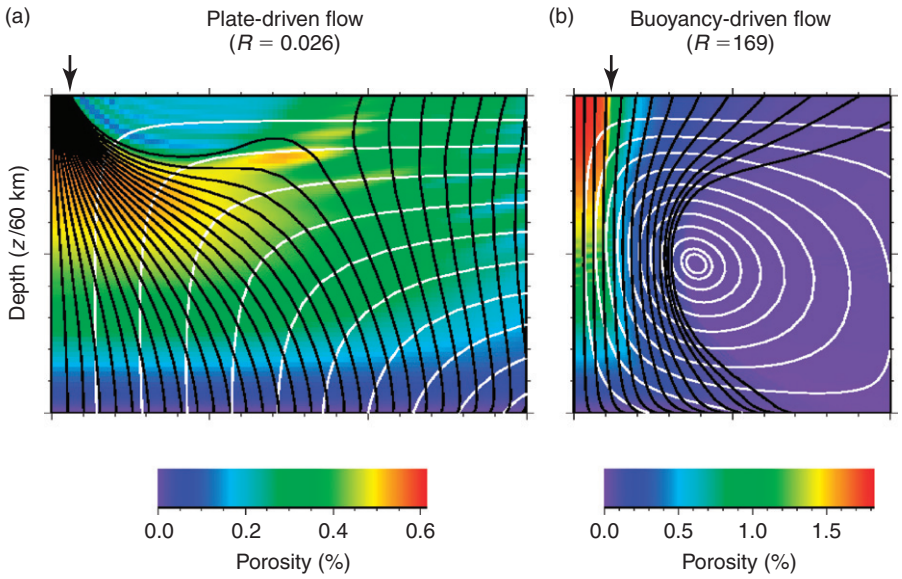

Figure 5 Predictions from 2-D numerical models of mantle flow (white streamlines), melt retention (shading), and pressure-driven melt migration (black streamlines). (a) Fast spreading with high mantle viscosity ($10^{20} - 10^{21}$ Pa s) impairs buoyant flow and leads to large pressure gradients, which draw melt from the broad melting zone toward the ridge axis. (b) Low mantle viscosity ($10^{18} - 10^{19}$ Pa s) allows the low-density, partially molten rock to drive buoyant upwelling, which focuses beneath the ridge axis and allows melt to flow vertically. Black arrows show the predicted width of ridge-axis magmatism, which is still much broader than observed. Figure provided by M. Spiegelman (pers. comm., 2007). Also, see Spiegelman M (1996) Geochemical consequences of melt transport in 2-D: The sensitivity of trace elements to mantle dynamics. *Earth and Planetary Science Letters* 139: 115–132.

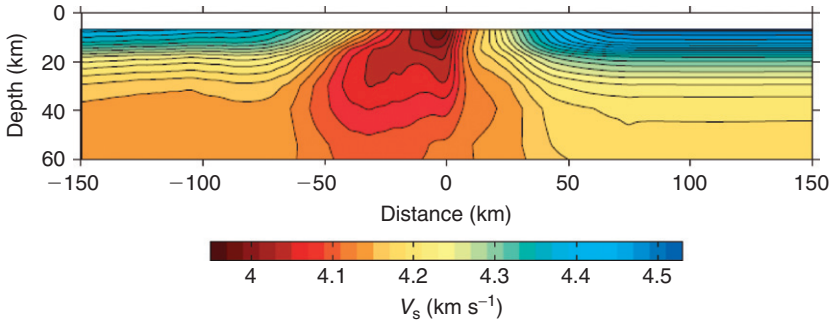

Figure 6 Cross-sectional tomographic image of the upper mantle shear wave velocity structure beneath the southern East Pacific Rise produced from Love wave data. Ridge axis is at $x = 0$ km. At the top of the figure the high-velocity lithospheric lid is clearly evident, as well as its thickening with distance from the ridge. The low-velocity zone beneath the ridge is consistent with the presence of high temperatures and some retained melt. Body wave and Rayleigh wave studies indicate that the low-velocity zone extends even wider below than what is shown here. Adapted from Dunn RA and Forsyth DW (2003) Imaging the transition between the region of mantle melting and the crustal magma chamber beneath the southern East Pacific Rise with short-period Love waves. *Journal of Geophysical Research* 108(B7): 2352 (doi:10.1029/2002JB002217), with permission from American Geophysical Union.

crustal thickness with decreasing spreading rate for rates $> c.$ 20 mm yr^{-1} must involve other processes.

A possible solution could have to do with the likelihood that the relative strengths of the plate-driven (i.e., kinematic) versus buoyancy-driven mantle upwelling change with spreading rate. Let us examine two end-member scenarios for mantle flow and melting. Case 1 considers a situation in which mantle flow is driven entirely kinematically by the separation of the lithospheric plates (Figures 3 and 5(a)). This passive flow scenario is predicted if the plate-driven component of flow overwhelms the buoyancy-driven part (i.e., the last term in eqn [1]). The other end-member possibility, case 2, considers a situation in which buoyant flow dominates over the plate-driven part. Lateral density variations, $\Delta\rho$, in the melting zone probably occur due to the presence of small amounts of melt, which has a lower density

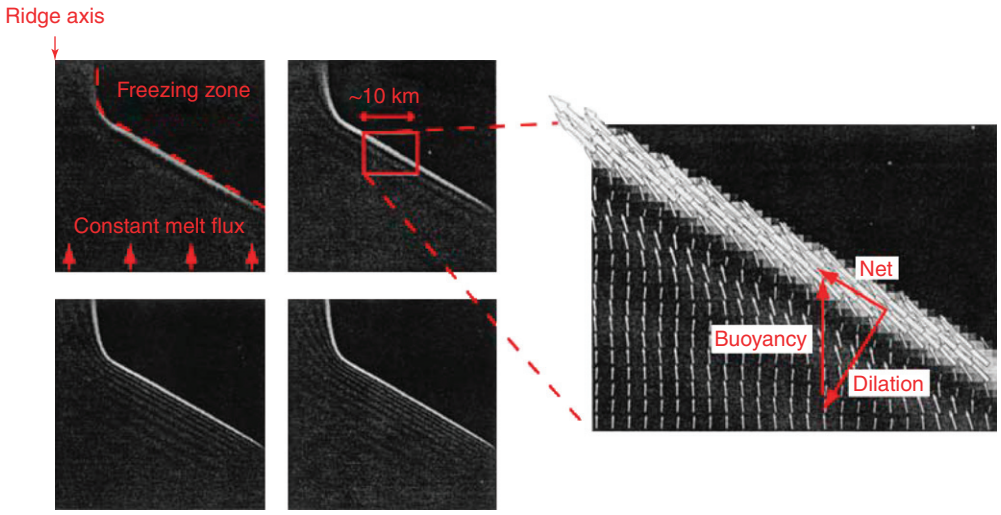

Figure 7 (Left) Cross-sections of a 2-D model of melt migration, with shading showing porosity (black = 0%, white = 3.5%) and at four different times, increasing clockwise from the upper left. A constant melt percolation flux rises through the bottom of the box. A 'freezing boundary' represents the cooler lithosphere which slopes toward the ridge axis (upper left). (Right) Enlarged portion of red box. The freezing boundary halts the rise of melt and diverts melt parallel to it. The net pressure gradient driving the flow is caused by the two components shown by the arrows. The freezing boundary generates porosity waves that propagate away from the boundary. These waves are predicted mathematically to arise from eqns [1], [2], and two others describing conservation of melt and solid mass. Modified from Spiegelman M (1993) Physics of melt extraction: Theory, implications and applications. *Philosophical Transactions of the Royal Society of London, Series A* 342: 23–41, with permission from the Royal Society.

than the solid. A positive feedback can occur between melting and buoyant flow, such that melting increases buoyancy and upwelling, which leads to further melting (Figure 5(b)). Returning to the weak dependence on spreading rate for rates $>20\,\mathrm{mm\,yr^{-1}}$; at least at fast-spreading rates, the plate-driven component of flow can be as strong or stronger than any buoyancy component. Thus, numerical models of fast-spreading ridges that do or do not include buoyancy predict similar crustal thicknesses and an insensitivity of crustal thickness to spreading rate (Figure 4). However, as spreading rate drops, buoyancy forces can become relatively important, so that – below slow–intermediate-spreading lithosphere – they generate 'fast' mantle upwelling. This fast upwelling is predicted to enhance melt production and compensate for the effects of surface cooling to shrink the melting zone; crustal thickness is therefore maintained as spreading rates decrease toward $\sim 20\,\mathrm{mm\,yr^{-1}}$.

Observational evidence for the relative importance of plate-driven versus buoyant flow is provided by studies of body and surface wave data along the EPR. Tomographic images produced from these data reveal a broad region of low seismic wave speeds in the upper mantle (Figure 6), interpreted to be the region of melt production. To date, there is little indication of a very narrow zone of low wave speeds, such as that predicted for buoyant upwelling zone as depicted by case 2 (Figure 5(b)). These findings support the predictions in Figure 4 that plate-driven flow is strong at fast-spreading ridges, such as the EPR.

At spreading rates less than $20\,\mathrm{mm\,yr^{-1}}$, however, the melting process appears to change dramatically. Here, melt flux is not proportional to spreading rate (Figure 4). At these ultraslow rates, crustal thickness drops rapidly with decreasing spreading rate, suggesting a nonlinear decrease in magma flux. A leading hypothesis suggests that the melt reducing effects of the top-down cooling and corresponding shrinkage of the melting zone overwhelm the melt-enhancing effects of any buoyancy-driven upwelling. Whatever the exact cause is, the large variability in crustal thickness seen at these spreading rates is one example of the large sensitivity of ridge-axis processes to surface cooling at slow or ultraslow spreading rates.

Melt Transport to Ridge Axes

How melt is transported upward from the mantle source to the ridge is another long-standing problem. Seismic studies of oceanic crust indicate that the crust is fully formed within a few of kilometers of the axis of a ridge, requiring either a very narrow melting zone beneath the ridge or some mechanism that focuses melts from a broader melting zone to a narrow region at the ridge axis.

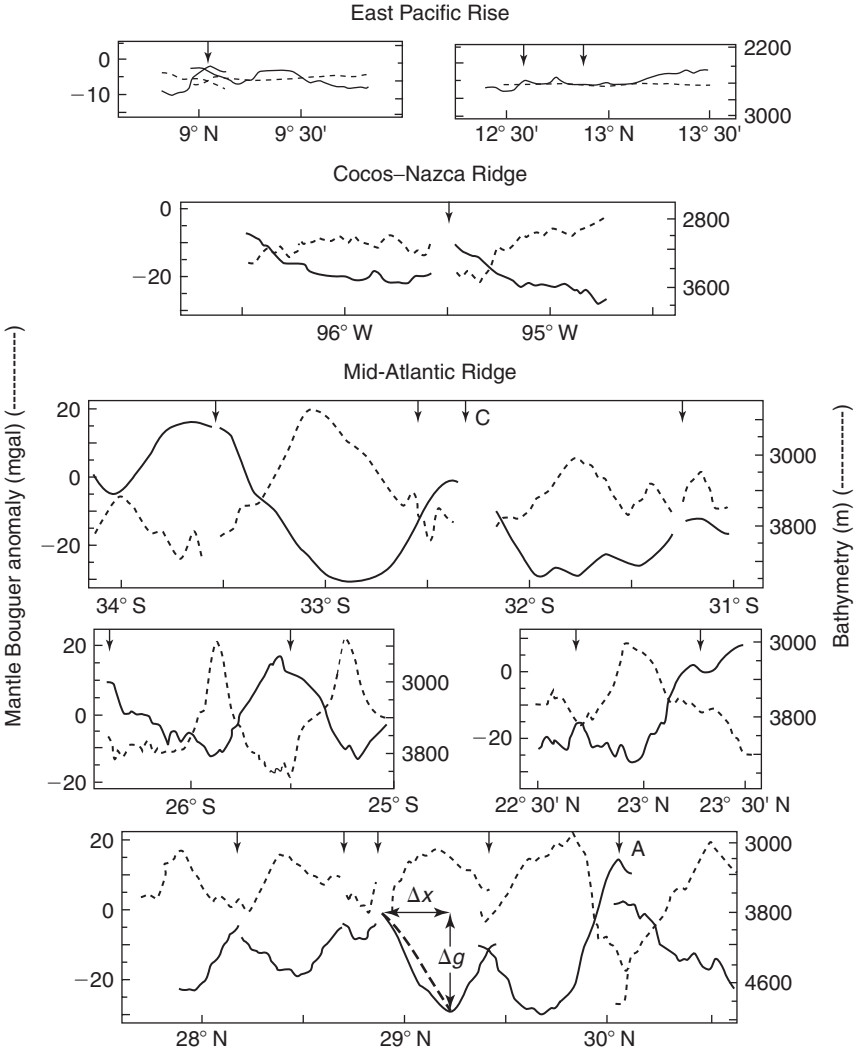

Figure 8 Profiles of seafloor depth (dashed lines) and mantle Bouguer gravity anomaly (solid lines) taken along the axes of various mid-ocean ridges (as indicated in the figure). Arrows mark various ridge-axis discontinuities. Note anticorrelation of gravity and bathymetry along the MAR, indicating shallower bathymetry and thicker crust near the centers of ridge segments. The East Pacific Rise is a fast-spreading ridge, the Cocos–Nazca Ridge (also called the Galapagos Spreading Center) spreads at an intermediate rate, and the MAR is a slow-spreading ridge. Adapted from Lin J and Phipps Morgan J (1992) The spreading rate dependence of three-dimensional mid-ocean ridge gravity structure. *Geophysical Research Letters* 19: 13–16, with permission from American Geophysical Union.

Laboratory experiments and theory show that melt can percolate through the pore space of the matrix (with volume fraction ϕ) in response to matrix pressure gradients ∇P. The Darcy percolation flux is described by

$$\phi(\mathbf{v} - \mathbf{V}) = -(k/\mu)\nabla P \qquad [2]$$

where $(\mathbf{v} - \mathbf{V})$ is the differential velocity of melt $\mathbf{v}$ relative to the matrix $\mathbf{V}$, μ is melt viscosity, and k is the permeability of the porous matrix. Equation [1] shows that ∇P is influenced by both melt buoyancy and matrix shear: melt buoyancy drives vertical percolation while matrix shear can push melt sideways. In mantle flow case 1, in which plate-driven flow dominates, the zone of melting is predicted to be very wide, requiring large lateral pressure gradients to divert melt 50–100 km sideways toward the ridge (Figure 5). For matrix shear to produce such large lateral gradients requires very high asthenospheric viscosities ($10^{20} - 10^{21}$ Pa s). When buoyant flow dominates (case 2), the melting zone is much narrower and the low viscosities (10^{18} 10^{19} Pa s) generate small lateral pressure gradients such that the melt rises mostly vertically to feed the ridge axis. Both of these cases, however, still predict zones of magmatism at the ridge axis that are wider than those typically observed.

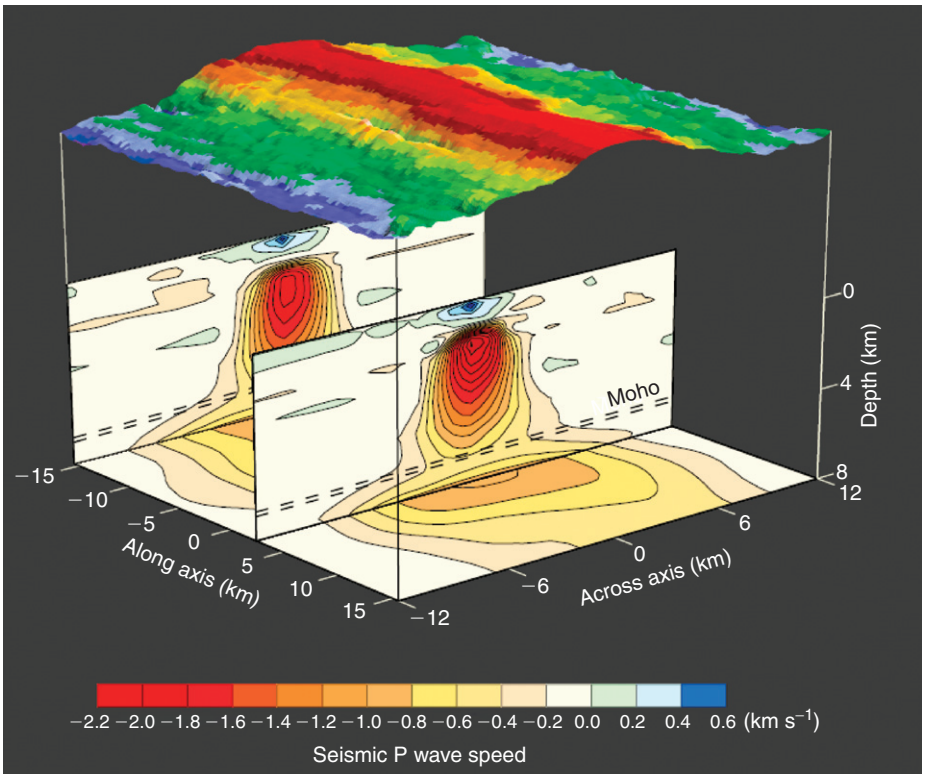

Figure 9 A perspective view of seafloor bathymetry and a seismic tomographic image of the East Pacific Rise (9° N latitude) magmatic system. The image is of the P wave velocity anomaly, relative to an average vertical velocity profile, contoured at 0.2 km s^{-1}. The vertical planes show the continuity of the crustal magmatic system beneath the ridge (the significant low-velocity region centered beneath the ridge). The deep horizontal plane is located in the mantle just below the crust and shows that the crustal low-velocity region extends downward into the mantle. The mantle velocity anomaly is continuous beneath the ridge, but shows variations in magnitude and location that suggest variations in melt supply. Adapted from Dunn RA, Toomey DR, and Solomon SC (2000) Three-dimensional seismic structure and physical properties of the crust and shallow mantle beneath the East Pacific Rise at 9° 30′ N. *Journal of Geophysical Research* 105: 23537–23555, with permission from the American Geophysical Union.

An additional factor that can help further focus melts toward the ridge is the bottom of the cold lithosphere, which shoals toward the ridge axis. Theoretical studies predict that as melt rises to the base of the lithosphere, it freezes and cannot penetrate the lithosphere (Figure 7). But the steady percolation of melt from below causes melt to collect in a high-porosity channel just below the freezing boundary. The net pressure gradient that drives melt percolation is the vector sum of the component that is perpendicular to the freezing front, caused by matrix dilation as melt fills the channel, and the vertical component caused by melt buoyancy. Consequently, melt flows along the freezing front, upward toward the ridge axis.

Regional and Local Variability of the Global Mid-Ocean Ridge System

Major differences in the regional and local structure of mid-ocean ridges are linked to the previously noted processes that influence asthenospheric flow and the heat balance in the lithosphere. One example that highlights a mid-ocean ridge's sensitivity to lithospheric heat balance is the overall shape or morphology of ridges at different spreading rates. At fast-spreading rates, the magmatic (heat) flux is high and this forms a hot crust with thin lithosphere. The mechanical consequences of both a thin lithosphere and relatively frequent magmatic intrusions to accommodate extension generate a relatively smooth, axial topographic ridge standing hundreds of meters above the adjacent seafloor (Figures 1 and 4). Slow-spreading ridges, however, have proportionally smaller magma fluxes, cooler crust, and thicker lithosphere. The mechanical effects of a thick lithosphere combined with less-frequent eruptions to accommodate extension cause the axes of slow-spreading ridges to be heavily faulted valleys, as deep as 2 km below the adjacent seafloor. Ridges spreading at intermediate rates show both morphologies, and appear to be sensitive to subtle fluctuations in magma supply. Seismic imaging of the crust reveals that melt

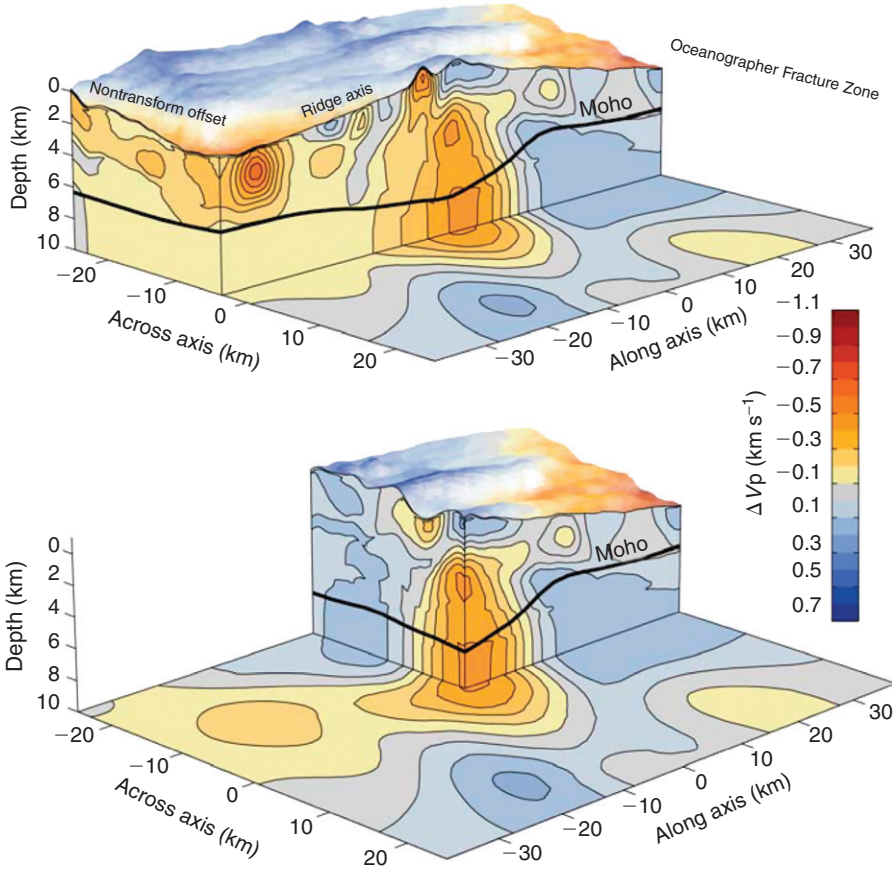

Figure 10 A perspective view of seafloor bathymetry and a tomographic image of the MAR (35° N latitude) magmatic system. The image is of the P wave velocity anomaly, relative to an average vertical velocity profile, contoured at 0.1 km s^{-1}. The vertical planes reveal partially molten bodies (the low-velocity regions), which are discontinuous beneath the ridge. The deep horizontal plane is located in the mantle just below the crust and shows that the crustal low-velocity region extends downward into the mantle. Crustal thickness is also greatest at the center of the ridge (black line labeled 'Moho'). The seismic image indicates that as magma rises in the mantle, it becomes focused to the center of the ridge segment where it then feeds into the crust. Adapted from Dunn RA, Lekic V, Detrick RS, and Toomey DR (2005) Three-dimensional seismic structure of the Mid-Atlantic Ridge at 35° N: Focused melt supply and non-uniform plate spreading. *Journal of Geophysical Research* 110: B09101 (doi:10.1029/2004JB003473), with permission from American Geophysical Union.

supply and crustal structure vary with spreading rate (Figure 4), geodynamic setting, as well as time.

Another major characteristic is the variability in topography, gravity, and crustal thickness as a function of distance along different mid-ocean ridges. Along individual segments of fast-spreading ridges, topography, gravity, as well as crustal thickness are remarkably uniform, varying by less then ~20% (Figures 8 and 9). Such relative uniformity probably indicates a steady magma supply from below as evident from seismic imaging of magma being stored over large distances along fast-spreading ridges (Figure 9). Quasi-steady-state crustal magmatic systems have been seismically shown to extend into the underlying mantle.

That said, the variability that is present between and along fast-spreading ridge segments reveals some important processes. Like all mid-ocean ridges, fast-spreading ridge segments are separated by large-qoffset fracture zones at the largest scale, and also by overlapping spreading centers (OSCs) at an intermediate scale. OSCs are characterized by the overlap of two *en echelon* ridge segments that offset the ridge by several kilometers. In one view, OSCs occur at the boundary between two widely separated, and misaligned, regions of buoyant mantle upwelling. An opposing model states that OSCs are mainly tectonic features created by plate boundary reorganization, below which mantle upwelling is primarily passively driven. A consensus on which hypothesis best explains the observations has not yet been reached.

At still finer scale, segmentation is apparent as minor morphologic deviations from axial linearity (or 'DEVALs') at intervals of 5–25 km. Individual DEVAL-bounded segments of the EPR are associated with higher proportions of melt in the crustal and

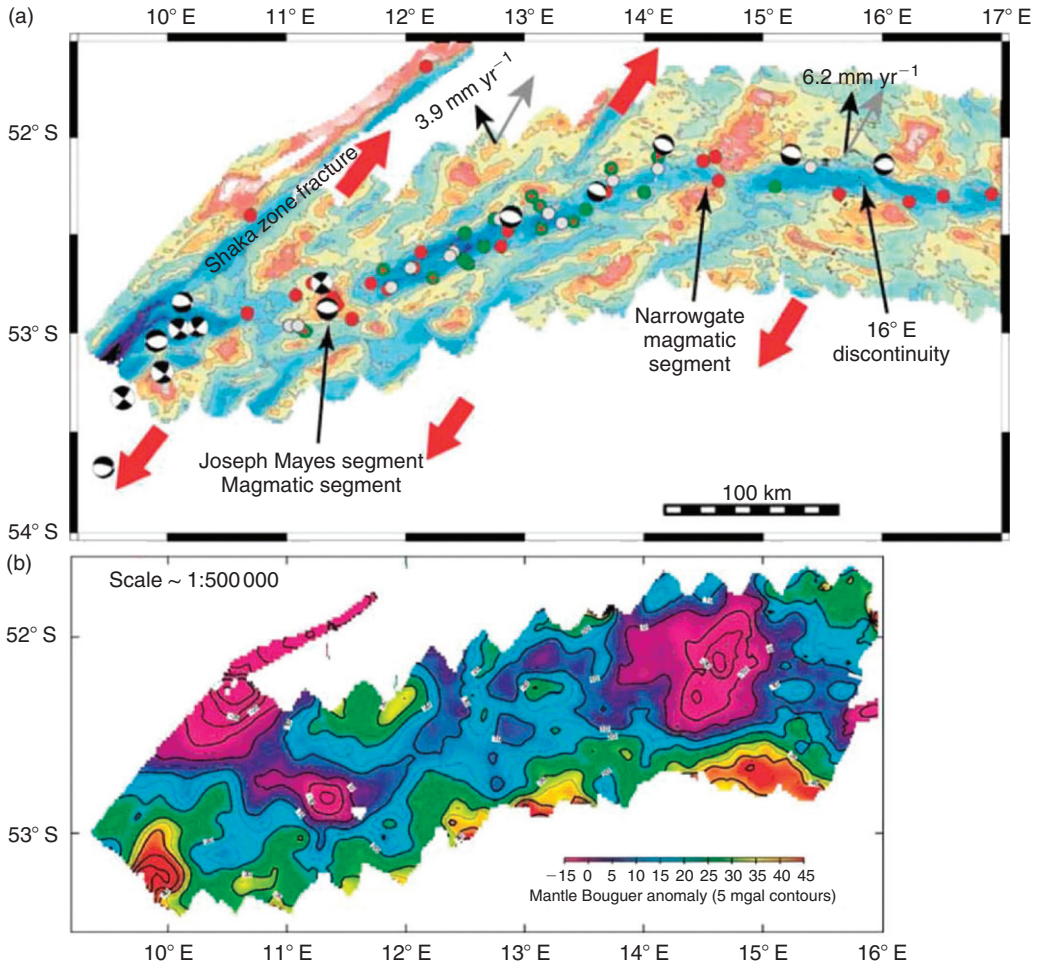

Figure 11 (a) Map of the Southwest Indian Ridge bathymetry (200-m contours). Ridge axis runs left to right across this figure. Large red arrows show relative direction of seafloor spreading (oblique to the ridge axis). Circles with black and white pattern indicate the locations and slip mechanisms of recorded earthquakes. Red and green dots indicate locations where crustal basaltic rocks and mantle peridotite rocks, respectively, were recovered. Significant amounts of mantle peridotite can be found at the seafloor along ultra-slow-spreading ridges. (b) Mantle Bouguer gravity anomaly. The large gravity lows signify thick belts of crust and/or low-density mantle, and correspond to regions where basalts have been predominantly recovered. Reprinted by permission from Macmillan Publishers Ltd: *Nature* (Dick HJB, Lin J, and Schouten H (2003) An ultraslow-spreading class of ocean ridge. *Nature* 426: 405–412), copyright (2003).

upper mantle magmatic system. This suggests that the melt flux from the mantle is locally greater between DEVALs than at the boundaries. The cause is controversial and may even have more than one origin. One possible origin is small-scale mantle diapirism that locally enhances melt production. Such a hypothesis is deduced from deformation fabrics seen in ophiolites, which are sections of oceanic lithosphere that are tectonically thrust onto continents. Alternatively, melt production can be locally enhanced by mantle compositional heterogeneity. Still other possibilities involve shallower processes such as variability in melt transport.

In stark contrast to fast-spreading ridges, slow-spreading ridges show huge variability in topography, gravity, and crustal thickness along individual spreading segments that are offset by both transform and nontransform boundaries (Figures 8, 10, and 11). The crust is usually thickest near the centers of ridge segments and can decrease by 50% or more toward segment boundaries (Figure 10). These and several other observations probably indicate strong along-axis variability in mantle flow and melt production. For example, a recent seismic study reveals a large zone in the middle to lower crust at the center of a slow-spreading ridge segment with very low seismic wave speeds. This finding is consistent with locally elevated temperatures and melt content that extend downward into the uppermost mantle. Although the observations can be explained by several different

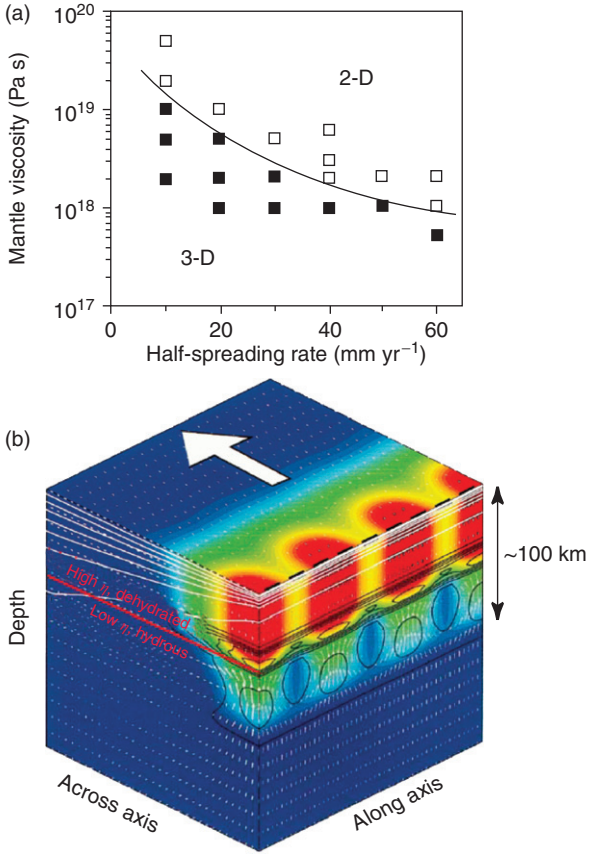

Figure 12 Predictions of a 3-D numerical model of mantle flow and melting. (a) Predicted variability in crustal production along the model ridge is characterized as 3-D or 2-D if the variability is, respectively, larger than or less than an arbitrary threshold. Along-axis variation increases with decreasing mantle viscosity and with decreasing spreading rate. (b) Perspective view showing retained melt (shading, varying from 0% far from the axis to 1.8% at centers of columnar zones), mantle flow (small white arrows of length proportional to flow rate), temperature (white contours), and melt productivity (black contours). The large white arrow depicts a plate spreading slowly at a rate of 12 mm yr^{-1} away from the plane of symmetry at the ridge axis (right vertical plane). Melt retention buoyancy generates convective mantle upwellings in the lower part of the melting zone where viscosities are low (below the red line). In the upper portion of the melting zone (above the red line), viscosity is high, owing to the extraction of water from the solid residue. In this zone, plate-driven mantle flow dominates. Thus, essentially all of the along-axis variability is generated in the lower half of the melting zone. It is the thickness of this lower zone of melting that controls the wavelength of variability. Wavelengths of 50–100 km are typical along the MAR. Adapted from Choblet G and Parmentier EM (2004) Mantle upwelling and melting beneath slow spreading centers: Effects of variable rheology and melt productivity. *Earth and Planetary Science Letters* 184: 589–604, with permission from American Geophysical Union.

mantle flow and melt transport scenarios, a predominant view supports the hypothesis that subridge mantle flow beneath slow-spreading ridges is largely influenced by lateral density variations.

Causes for the major differences in along-axis variability between fast- and slow-spreading ridges have been explored with 3-D numerical models of mantle convection and melting. Models of only plate-driven flow predict that the disruption of the ridge near a segment offset both locally reduces upwelling and enhances lithosphere cooling beneath it, both of which tend to somewhat reduce melt production near the offset. For a given length of segment offset, the size of the along-axis variability is smallest at the fastest spreading rates and increases with decreasing spreading rate. This prediction is broadly consistent with the observations; however, such models still underpredict the dramatic variability observed along many segments of slow-spreading ridges.

Again, a consideration of both plate- and buoyancy-driven flow provides a plausible solution. In the direction parallel to the ridge axis, variations in density can be caused by changes in temperature, retained melt, as well as solid composition due to melt extraction (melting dissolves high-density minerals and extracts high-density elements like iron from the residual solid). All three sources of buoyancy are coupled by the energetics and chemistry of melting and melt transport. As discussed above, models of fast-spreading systems predict plate-driven flow to be most important such that buoyancy causes only subtle along-axis variations in melting (Figure 12). As spreading rate decreases, the relative strength of buoyant flow increases as does the predicted variability of melt production. Models that include buoyancy more successfully predict typical amplitudes of variations along slow-spreading ridges.

Even more dramatic melt supply variations are observed at a few locations along ridges, which include the MAR at Iceland and near the Azores Islands, the Galapagos Spreading Center near the Galapagos Archipelago, and the EPR near Easter Island (Figure 1). These regions occur where 'hot spots' in the mantle produce so much magmatism that islands are formed. Iceland in fact is a location where a mid-ocean ridge is actually exposed above sea level. These 'hot-spot-influenced' sections of mid-ocean ridges show elevated topography and enhanced crustal thickness over distances of many hundreds of kilometers. The most likely cause for these features are anomalously hot, convective upwellings that rise from depths at least as deep as the base of the upper mantle. Fluid dynamical studies show that plumes of rising mantle can arise from hot thermal boundary layers such as the core mantle boundary. When these hot upwellings eventually rise to the lithosphere, they expand beneath it and can enhance volcanism over large distances (Figure 13).

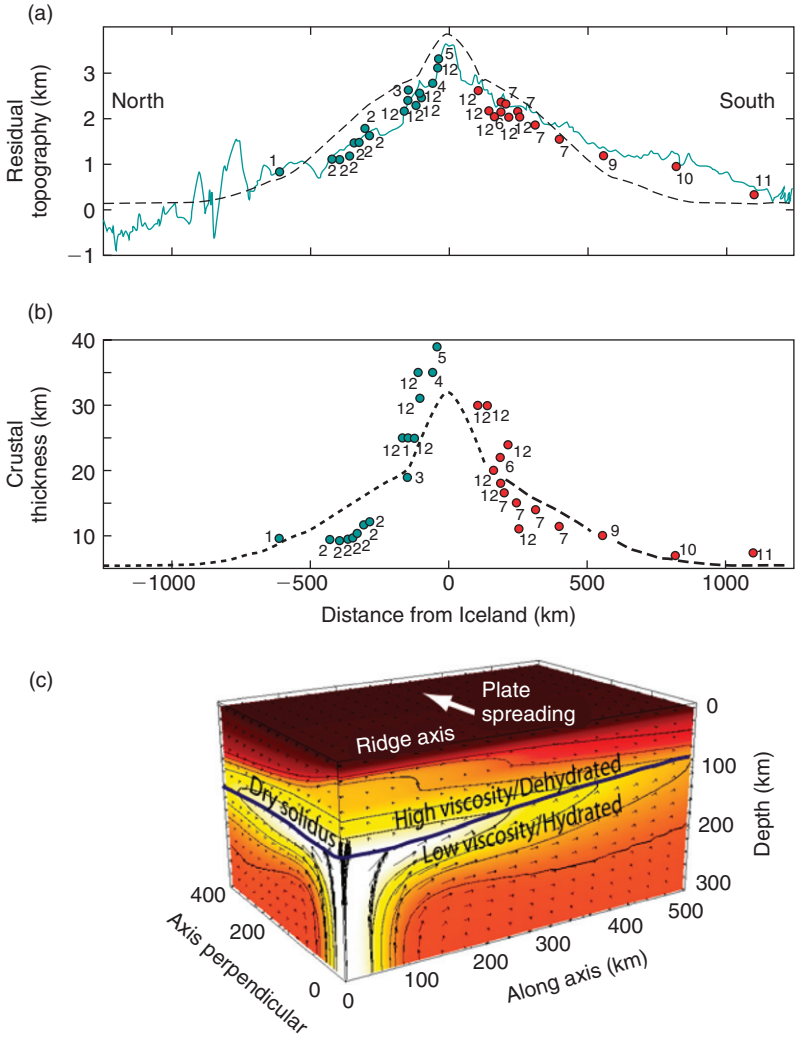

Figure 13 (a) Observed residual topography (solid curve and circles) and (b) crustal thickness of Iceland and the MAR, compared to the predictions of a 3-D model of a hot mantle plume rising beneath the ridge (dashed). (c) Perspective view of potential temperatures (white $>c.$ 1500 °C) within the 3-D model. The vertical cross sections are along (right) and perpendicular (left) to the ridge. Viscosity decreases with temperature and increases at the dry solidus by 10^2 because water is extracted from the solid with partial melting. Thermal buoyancy causes the hot plume material to spread hundreds of kilometers along the MAR away from Iceland. Crustal thickness is predicted to be greatest above the hot plume and to decrease away from Iceland due to decreasing temperatures. Reproduced from Ito G and van Keken PE (2007) Hot spots and melting anomalies. In: Bercovici D (ed.) *Treatise in Geophysics*, *Vol. 7*: *Mantle Dynamics*. Amsterdam: Elsevier, with permission from Elsevier.

So far, we have discussed characteristics of the mid-ocean ridge system that are likely to be heavily influenced by differences in heat transport and mantle flow. At the frontier of our understanding of mantle processes is the importance of composition. Studies of seafloor spreading centers at back of the arcs of subduction zones reveal how important mantle composition can be to seafloor creation. For example, the Eastern Lau Spreading Center is characterized by rapid along-strike trends in many observations that are contrary to or unseen along normal mid-ocean ridges. Contrary to the behavior of mid-ocean ridges, as spreading rate increases along the Eastern Lau back arc spreading system from a slow rate of $\sim 40\,\mathrm{mm\,yr^{-1}}$ in the south to an intermediate rate of $\sim 95\,\mathrm{mm\,yr^{-1}}$ in the north, the ridge axis changes from an inflated axial high to a faulted axial valley and the evidence for magma storage in the crust disappears. Coincident with this south-to-north variation, the crustal composition changes from andesitic to tholeiitic and isotopic characteristics change from that of the Pacific domain to more like that in the Indian Ocean.

It is hypothesized that many of the along-strike changes along the Eastern Lau Spreading Center are produced by variable geochemical and petrological

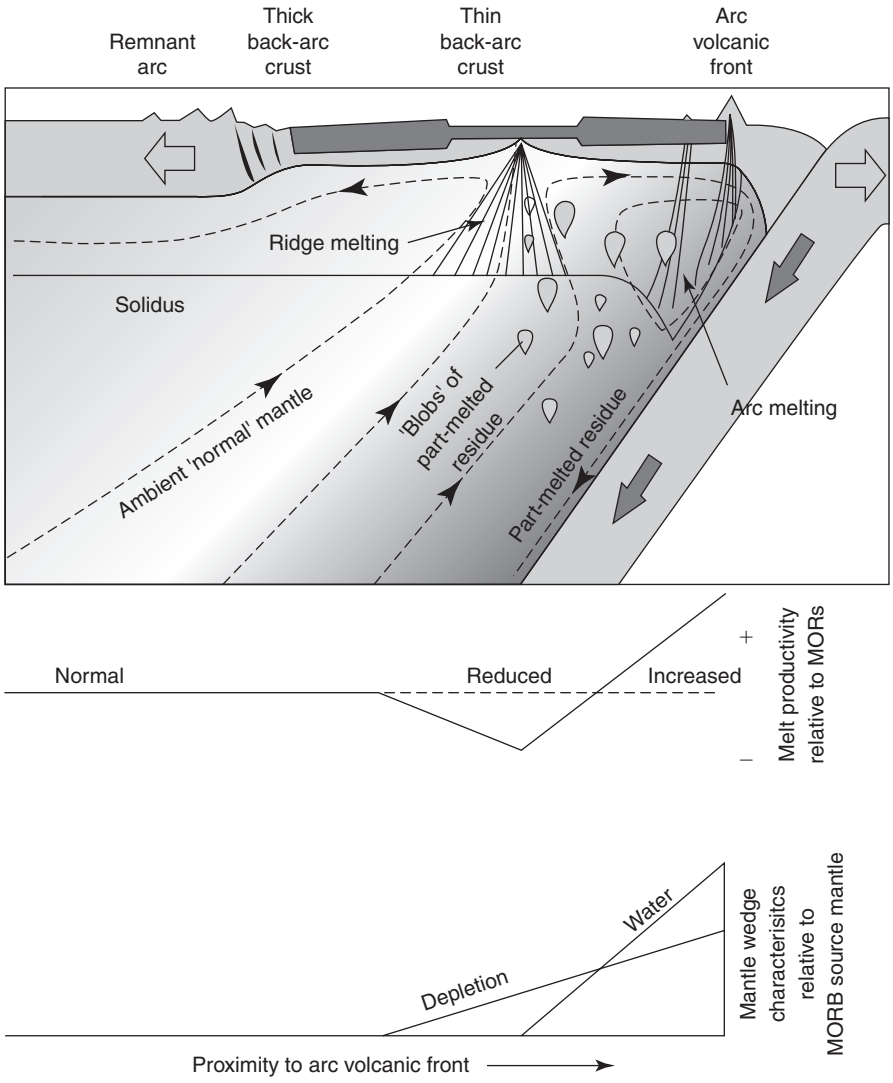

Figure 14 Mantle composition in the wedge above a subducting slab can significantly affect melting beneath back-arc spreading centers. In this scenario, buoyant (partially melted) residual mantle from the arc region is rehydrated by water expelled from the subducting plate, becomes less viscous, and rises into the melting regime of the spreading center, where (because it has already been partially melted) it reduces the total melt production (middle panel). Arc volcanism occurs closer to the subduction zone and originates as fluids percolate from the subducting slab up into the hot mantle wedge and cause melting by reducing melting temperature. If seafloor spreading were closer to this arc melting zone, it would likely form 'thick back-arc crust' and an axial morphology that resembles fast spreading ridges even though spreading here could be slow. Bottom curves schematically show melt depletion and hydration trends in the mantle wedge and their hypothesized effects on the ridge melt productivity with distance from the arc volcanic front. MORS, mid-ocean ridges; MORB, mid-ocean ridge basalt. Adapted from Martinez F and Taylor B (2006) Modes of crustal accretion in back-arc basins: Inferences from the Lau Basin. In: Christie DM, Fisher CR, Lee S-M, and Givens S (eds.) *Geophysical Monograph Series 166: Back-Arc Spreading Systems: Geological, Biological, Chemical, and Physical Interactions*, pp. 5–30 (10.1029/l66GM03). Washington, DC: American Geophysical Union, with permission from American Geophysical Union.

inputs influenced by subduction (Figure 14). From south to north, the distance of the ridge from the Tonga arc increases from 30 to 100 km and the depth to the underlying slab increases from 150 to 250 km. To the south, melt production is most likely enhanced by the proximity of the ridge to the arc which causes the ridge to tap arc volcanic melts (slab-hydrated); whereas to the north, melt flux is probably reduced by the absence of arc melts in the ridge melting zone, but in addition, the mantle flow associated with subduction could actually deliver previously melt-depleted residue back to the ridge melting zone. Yet farther to the north, the ridge is sufficiently far away from the slab, such that it taps 'normal' mantle and shows typical characteristics of mid-ocean spreading centers. Similar hypotheses have been formed for other back-arc systems.

Summary

The global mid-ocean ridge system is composed of the divergent plate boundaries of plate tectonics and it is where new ocean seafloor is continually created. Of major importance are the effects of plate motion versus buoyancy to drive asthenospheric upwelling, the balance between heat advected to the lithosphere versus that lost to the seafloor, as well as mantle compositional heterogeneity. Such interacting effects induce variations in the thickness of crust as well as local structural variability of mid-ocean ridge crests that are relatively small at fast-spreading ridges but become more dramatic as spreading decreases. Through examining this variability geoscientists are gaining an understanding of mantle convection and chemical evolution as well as key interactions with the Earth's surface.

See also

Mid-Ocean Ridge Geochemistry and Petrology. Mid-Ocean Ridge Seismic Structure. Mid-Ocean Ridge Seismicity. Mid-Ocean Ridge Tectonics, Volcanism, and Geomorphology. Seamounts and Off-Ridge Volcanism.

Further Reading

Buck WR, Lavier LL, and Poliakov ANB (2005) Modes of faulting at mid-ocean ridges. *Nature* 434: 719–723.

Choblet G and Parmentier EM (2004) Mantle upwelling and melting beneath slow spreading centers: Effects of variable rheology and melt productivity. *Earth and Planetary Science Letters* 184: 589–604.

Dick HJB, Lin J, and Schouten H (2003) An ultraslow-spreading class of ocean ridge. *Nature* 426: 405–412.

Dunn RA and Forsyth DW (2003) Imaging the transition between the region of mantle melting and the crustal magma chamber beneath the southern East Pacific Rise with short-period Love waves. *Journal of Geophysical Research* 108(B7): 2352 (doi:10.1029/2002JB002217).

Dunn RA, Lekic V, Detrick RS, and Toomey DR (2005) Three-dimensional seismic structure of the Mid-Atlantic Ridge at 35° N: Focused melt supply and non-uniform plate spreading. *Journal of Geophysical Research* 110: B09101 (doi:10.1029/2004JB003473).

Dunn RA, Toomey DR, and Solomon SC (2000) Three-dimensional seismic structure and physical properties of the crust and shallow mantle beneath the East Pacific Rise at 9° 30′ N. *Journal of Geophysical Research* 105: 23537–23555.

Forsyth DW, Webb SC, Dorman LM, and Shen Y (1998) Phase velocities of Rayleigh waves in the MELT experiment on the East Pacific Rise. *Science* 280: 1235–1238.

Huang J, Zhong S, and van Hunen J (2003) Controls on sublithospheric small-scale convection. *Journal of Geophysical Research* 108: 2405 (doi:10.1029/2003 JB002456).

Ito G and van Keken PE (2007) Hot spots and melting anomalies. In: Bercovici D (ed.) *Treatise in Geophysics*, *Vol. 7*: *Mantle Dynamics*. Amsterdam: Elsevier.

Lin J and Phipps Morgan J (1992) The spreading rate dependence of three-dimensional mid-ocean ridge gravity structure. *Geophysical Research Letters* 19: 13–16.

Martinez F and Taylor B (2006) Modes of crustal accretion in back-arc basins: Inferences from the Lau Basin. In: Christie DM, Fisher CR, Lee S-M, and Givens S (eds.) *Geophysical Monograph Series 166: Back-Arc Spreading Systems: Geological, Biological, Chemical, and Physical Interactions*, pp. 5–30. Washington, DC: American Geophysical Union (doi:10.1029/l66GM03).

Phipps Morgan J, Blackman DK, and Sinton JM (eds.) (1992) *Geophysical Monograph 71: Mantle Flow and Melt Generation at Mid-Ocean Ridges*, p. 361. Washington, DC: American Geophysical Union.

Phipps Morgan J and Chen YJ (1993) Dependence of ridge-axis morphology on magma supply and spreading rate. *Nature* 364: 706–708.

Shen Y, Sheehan AF, Dueker GD, de Groot-Hedlin C, and Gilbert H (1998) Mantle discontinuity structure beneath the southern East Pacific Rise from P-to-S converted phases. *Science* 280: 1232–1234.

Spiegelman M (1993) Physics of melt extraction: Theory, implications and applications. *Philosophical Transactions of the Royal Society of London, Series A* 342: 23–41.

Spiegelman M (1996) Geochemical consequences of melt transport in 2-D: The sensitivity of trace elements to mantle dynamics. *Earth and Planetary Science Letters* 139: 115–132.

Stein CA and Stein S (1992) A model for the global variation in oceanic depth and heat flow with lithospheric age. *Nature* 359: 123–129.

Relevant Websites

http://www.ridge2000.org
– Ridge 2000 Program.